Proceedings of 2021 IEEE
International Conference on Mechatronics and Automation
August 8 - 11, Takamatsu, Japan

Mechanism Design, Kinematic and Hydrodynamic Simulation of a Wave-driven Amphibious Bionic Robot

Zhongyin Zhang[1,2] , Liwei Shi[1,2*] , Shuxiang Guo[1,2,3*] , He Yin[1,2] , Ao Li [1,2] , Pengxiao Bao[1,2] , Meng Liu[1,2]

[1]*Key Laboratory of Convergence Medical Engineering System and Healthcare Technology, the Ministry of Industry and Information Technology, School of Life Science, Beijing Institute of Technology, No.5, Zhongguancun South Street, Haidian District, Beijing 100081, China*

[2]*Key Laboratory of Biomimetic Robots and Systems, Ministry of Education, Beijing Institute of Technology, No.5, Zhongguancun South Street, Haidian District, Beijing 100081, China*

[3]*Faculty of Engineering, Kagawa University, 2217-20 Hayashi-cho, Takamatsu, Kagawa, Japan*

E-mails: zhangzhongyin@bit.edu.cn; shiliwei@bit.edu.cn; guoshuxiang@bit.edu.cn;

* Corresponding author

***Abstract* -Amphibious robots has been a hot research direction. They can not only save cost, but also improve the efficiency of kinds of jobs and cope with various complex environments. Compared with the common multi-steering gear oscillating fins robot, this paper uses the 30 degrees of the opposite angle of the 12 groups, which can produce the fish fins of a similar function. The 12 drivers are connected to the 12 units of the lever, which can be driven by a single steering machine. The existing amphibious robots are mostly used by several steering gear to drive the fins, the structure redundancy and the control circuits are complex, and most of them are steering the direction of the rudder, which needs to be designed to turn to the body. Therefore, the fin components on both sides of this robot are driven by a corresponding steering machine, which is used to achieve acceleration and turn, and the adjustment mechanism of the fish fin is set up to realize the transformation of amphibians. Using Adams to simulate the motion of the rocker, the acceleration curve on the component is obtained. The corresponding speed and pressure curves were obtained by using fluent to simulate the fish fins of different phase angles. The research results are of great significance to the design and control of multi-modal motion in the next generation flexible underwater navigation and robot.**

Index Terms - Mechanism Design, Kinematic simulation, Wave-driven amphibious bionic robot.

I. INTRODUCTION

In recent years, colleges and universities have begun to pay attention to scientific research in the Marine field. The urgent exploration of Marine resources has stimulated people's research and exploration on underwater robots. Most of the underwater robots are propellers, but such propellers have disadvantages such as large volume, high noise and high energy consumption. The ray robot with the pectoral fin swing as the propulsion mode has significant advantages in mobility, flexibility and adaptability to amphibious environment [1~3].

BCF(caudal fin) and MPF(central fin) are two common propulsion modes of fish bionic robots. The skate drive belongs to the central fin drive [4].Yang Shaobo [5]took the bull nose ray as the research object, and the two sides of the pectoral fins were driven by eight steering gear. By imitating the motion pattern of pectoral fins, the desired effect has been achieved. Wang Tianmiao [6]also took the bull nose ray as the research object and added the caudal fin, which can realize free turning and greatly improve the swimming performance. Wang Yangwei [7] takes manta rays as the research object and uses shape memory alloy as the driving material.

Low [8] takes the manta ray as the research object, and through the multi-steering gear drive, it can achieve the same autonomous swimming as the ray basically. Chen [9] took ray as the research object and used lead zirconate titanate inorganic material as the drive, which could well simulate the swimming form of ray, but the swimming speed was relatively slow. EvoLogics [10] has built a robot that looks like a ray using artificial muscle technology. The driving mode of pneumatic tendon can achieve better movement.

A fish-like long-fin undulating propulsion underwater vehicle was developed in the university of national defense science and technology, and a motion control algorithm based on iterative learning was proposed to maintain a high steady propulsion speed [11].

The Institute of Automation of the Chinese Academy of Sciences has developed a kind of imitated growth fin robotic fish, which is propelled by a pair of undulating pectoral fins [12]. In the second generation of robotic fish, multi-mode motion control such as forward and backward motion control, directional control of fixed depth and closed-loop position control of path point tracking control have been realized.

Inspired by legged animals, the amphibious robot Aqua was developed by McGill University in Canada in 2005 to meet the application requirements of underwater industrial scene detection [13]. The six-paddle type foot is designed to meet the requirements of 6-DOF swimming and underwater walking. The size of the robot is 65cm×45cm×13 cm, the total body weight is 18 kg, the maximum dive is 14 m, and the maximum underwater sailing speed is 0.4 m/s. The front part of the robot is equipped with binocular eyes to realize the target positioning and target tracking functions. In 2015, Yeungnam University [14] in South Korea designed a six-legged amphibious robot using lizards as bionic prototypes.

The legs of the robot are driven by connecting rods and the feet are ball-shaped to provide buoyancy. The size of the robot is 40.8cm×23cm×12 cm, and the maximum walking speed on land and water is 0.77 m/s and 0.48 m/s, respectively. In 2014, RoboterP [15], an amphibious robot, was developed at the University of Maryland. It uses a quadruped compound drive mode, paddling in water with four driven blades, and walking in a diagonal trot gait with leg joint fulcrum on land. In this study, the material of the blade and the joint size of the leg were analyzed and optimized by using the finite element tool. In 2016, the University of Science and Technology of China (USTC) designed Amphihex-I [16], a six-legged amphibious robot, using multi-joined deformable fins. Hexapod deformation on land such as driving wheel, walking over obstacles; In the water, flippers swing and paddle. In 2018, a new variable strength leg with a rigid fan-shaped leg structure was modified and named Amphihex-II [17] to improve the robot's performance on land and in water. The maximum velocity on land and in water is 0.16m /s and 0.18BL /s.

In 2017, Professor Sun Hanxu's research [18] and development team from Beijing University of Posts and Telecommunications developed a spherical robot with a diameter of 0.4m, a mass in the air of 25kg, a maximum load of 4kg, using the robot's internal flywheel, gravity pendulum and propeller drive to achieve a full range of underwater movement, and a top speed of 1.4m/s. In 2011, a team from Harbin Engineering University [19] developed a Spherical Underwater robot. The air mass is about 7kg, through three groups of vector jet machine configuration into dynamic force, can show the four degrees of self-movement of machine under the water. In 2012, the team launched the improved underwater spherical robot SUR-II [20] on the basis of the previous generation robot. It adopts a semi-open spherical structure design, three groups of vector water jet propulsion.

From the above study, it can be seen that the wheel-leg mechanism has a high degree of freedom, but it requires a high control program, and the land walking speed is very slow. Spherical robot with many functions and is easy to control and seal, but bulky structures are only good at moving in water. It is obvious that the commonly used amphibious robots adopt different walking structures and modes on land and in water, and the switching mode is more complicated.

In this paper, we design a kind of driving structure shared by both land and water. There is no need to switch between the two movement structure. The structure is simpler and reliable and it is easy to waterproof and seal. The first chapter mainly introduces the overall structure design, including the driving structure and angle adjustment structure. In the second chapter, the kinematic simulation of the driving mechanism is carried out to obtain the acceleration of the driving rod at different driving speeds. In the third chapter, a river basin is set to simulate the fluid flow of fins in 12 different states. The pressure and velocity cloud maps are obtained. The resistance and buoyancy of fins in the river basin are analyzed and studied. Finally, the paper verifies the feasibility of the structure and will provide reference data for the follow-up research.

II. Ray Structure Design

As can be seen from the fig.1, the drive structure and the fin are symmetrical. Each fin is composed of 24 pairs of drive disks and 12 horizontal swing rods. The swing rods are connected by rubber to form a wavy fin. Each set of driving disks has an Angle of 30 degrees, and the 12 sets form exactly a 360-degree cycle. All the disks rotate at the same speed in sync, and the swinging fins create waves on either side that propel the whole structure forward.

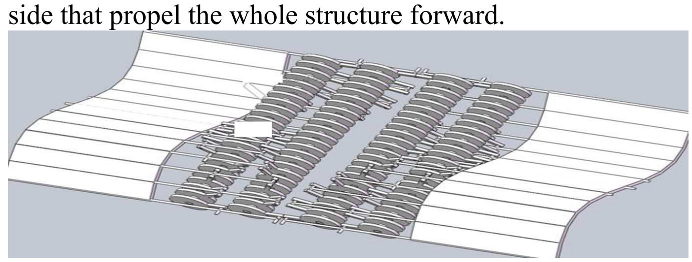

Fig. 1 Overall structural design

A. *Bindiny mechanism*

Mechanical structure mainly introduces the rocker driving mode and amphibious conversion structure.12 fin oscillating rods driven by 12 groups of crank rocker mechanism, as is shown above, there are two holes on each of the fixed bracket, used to fix two axis of wafer, support the four crank on one side of the equal length and parallel, holder of a four crank end can have holes, four holes used to connect swinging rod, the effect of swinging rod is not only driven fins, have an important role in the same side is to ensure that the consistency of the crank movement.

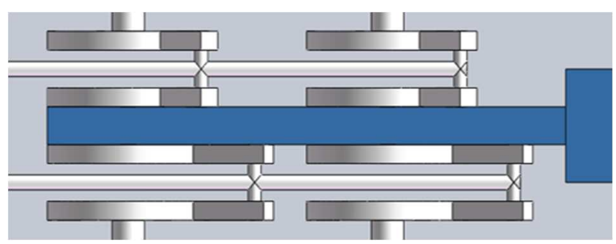

Fig. 2 The composition of the driving mechanism

B. *The general structure of a fish fin*

As can be seen from the above fig.2, the crank difference Angle on both sides of the bracket is fixed at 30 degrees. The 13 groups of cranks just ensure that the crank covers the whole circumference and forms a cycle. In addition, from the perspective of the fin, it can be seen that the fin supported by the swinging rod also forms a cycle similar to the sine function.

Each swing rod is connected with a 6mm thick rubber sheet, which can adapt to the change of the distance between the swing rods. The elasticity of rubber can also be used to reduce the swing of the whole mechanism, so as to achieve the purpose of noise reduction.

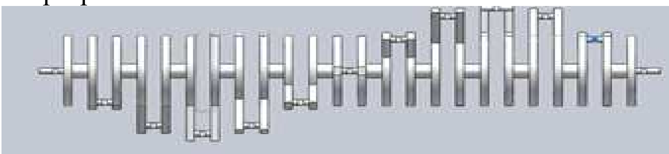

(a) transmission mechanism

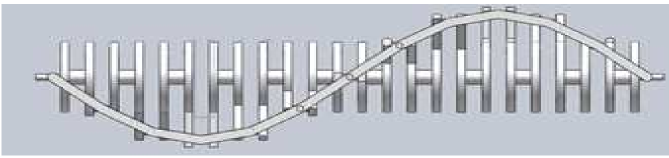

(b) transmission mechanism and fin

Fig. 3 A swing rod connected with rubber

C. *Angle adjusting mechanism*

Fig.4 shows the Angle adjustment mechanism, with a row of supports on the left and right sides, and two cranks in the middle to adjust the Angle between the supports, which can vary from 0 to 38 degrees. When the ray moves through the water, the scaffold is arranged symmetrically, at an Angle of 0 degrees, and the overall plane of the fin is horizontal. When the ray moves on land, the Angle increases to 38 degrees and the end of the fin lands. The ray uses friction between the rubber and the ground to move forward. Because rubber is adaptable, the ray can move quickly through ice and snow.

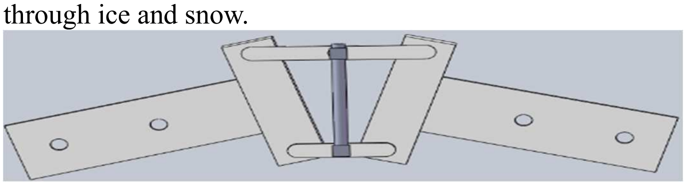

(a)maximum Angle state

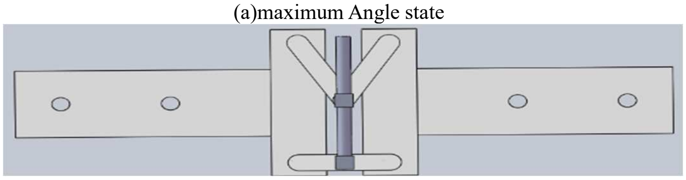

(b) minimal Angle state

Fig. 4 Angle adjusting mechanism

III. Kinematic Simulation Of Ray Mechanism

In order to verify the feasibility of the mechanical structure, we added connections and drives to the original model to verify the feasibility of the structure. In addition, the motion of the structure can be inferred through data from the simulation.

A. *Equations*

The kinematic model of undulating fins has been established in the ruled surface as follows [21]:

$$p_{x_i}(r_i, s_i, t) = s_i \quad (1),$$

$$p_{y_i}(r_i, s_i, t) = r_i \cdot d \cdot \cos[\theta_{m,i} \cdot sin\left(\frac{2\pi}{T_i} t + \sigma_i \frac{2\pi}{\lambda_i} s_i + \emptyset_i\right)] \quad (2),$$

$$p_{y_i}(r_i, s_i, t) = r_i \cdot d \cdot \sin[\theta_{m,i} \cdot sin\left(\frac{2\pi}{T_i} t + \sigma_i \frac{2\pi}{\lambda_i} s_i + \emptyset_i\right)] \quad (3),$$

$$0 \le s_i \le L, 0 \le r_i \le 1,$$

where i =1, 2, L is the fin length, d is the uniform length of each fin ray, $\theta_{m,i}$ is the maximal undulation angle, T_i is the undulating period, λ_i is the undulating wavelength, $\emptyset_i$ is the initial phase and σ_i decides the direction of wave traveling.

B. *Result*

If the 12 groups of crank rocker mechanism and fish fin simulation, the process will be more complex, now choose 2 pairs of rocker from them for simulation. Because of the different trajectories of each point on the disk, the motion of the connected swing rod is studied. When the disk swings at speeds of 90°, 180°, 360° and 720°/s, the acceleration in the direction of the journal of the swing rod is measured.

Acceleration(m/s^2)

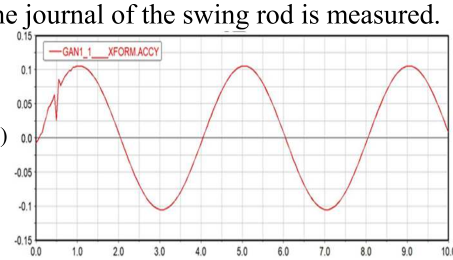

Time(s)

(1) When swing speed is 90°/s

Acceleration(m/s^2)

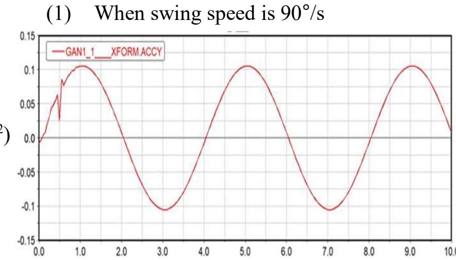

Time(s)

(2) When swing speed is 180°/s

Acceleration(m/s^2)

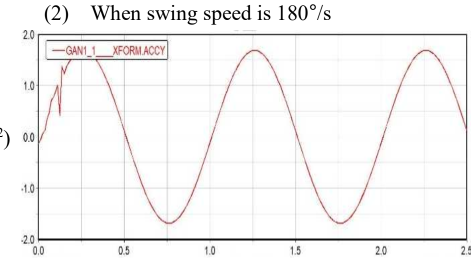

Time(s)

(3) When swing speed is 360°/s

Acceleration(m/s^2)

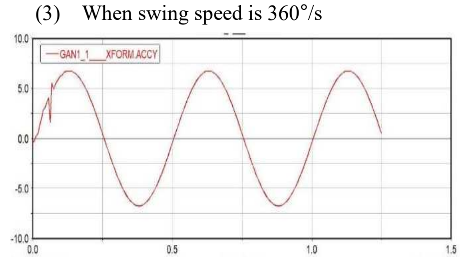

Time(s)

(4) When swing speed is 720°/s

Fig. 5 Accelerations for different oscillating velocities

From these four figures, it can be seen that the acceleration of the swing rod presents the shape of sine function, which is consistent with the theoretical calculation. When the angular velocities of the disks are 90, 180, 360, and 720 degrees /s, the maximum accelerations are 0.1, 0.4, 1.6 and 6.4m/s^2. In addition, the phase of the acceleration will also be the same because the initial Angle is the same. fig.5 shows the change of fin angular velocity at different speeds of the steering gear. The angular velocity of the fin changes periodically with time. With the increase of the rotating speed of the steering gear, the motion velocity of the fin increases gradually. And when the crankshaft journal moves to the position perpendicular to the fin slider, the fin just moves to the upper and lower limit positions, that is, the maximum swing Angle, at this time the angular velocity is zero. When moving to a parallel position, the swing Angle is zero and the angular velocity of the fin is the maximum. This is the result derived from the previous formula. The rationality of the mechanism is verified.

IV. Fin Hydrodynamic Simulation

A dynamic model is created for the fin part. The fin surface looks like a regular sine function from the side, and its motion equation is:

$$y = A \cdot \sin(kx - wt) \qquad (4),$$

In the formula, $k = 2\pi/\lambda$; $w = 2\pi f$; x, y is the coordinate of any point of the fin. T is the time of exercise, λ is the length of the traveling wave, f is the frequency of the traveling wave, A is the amplitude of fin fluctuation [22].

As the ray moves, torque is applied to the first disk by the steering gear, which then drives the next disk through a swing rod. We can get the positions of the swing bars at different times, connect the swing bars with rubber, and simulate. Since the fins are symmetrical on both sides, only one side is considered.

Fig.1 shows the overall frame of the structure, with the wavy fins on both sides showing different shapes as the disk is driven. Since the shape changes periodically, in order to facilitate the study, fins at 12 time points within the cycle were selected for the study, and the phase difference of each fin was 30 degrees. As shown in fig.6, rubber is used to form fins between swinging rods, which means that the shapes of fins are different at different times. In order to facilitate the study, the Angle between the first crank and bracket is set to 12 angles, such as 0 °,30 °, 60 °,⋯ ,330 °, and 12 fins in the initial state are obtained.

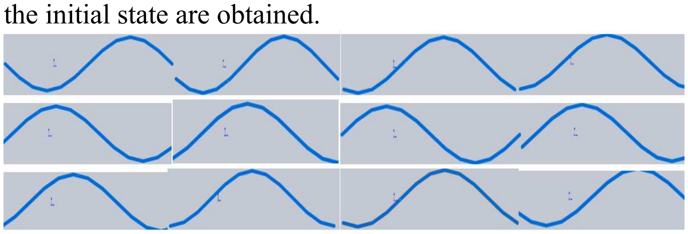

Fig. 6 12 fins in the initial state

A. Analysis of pressure on fin surface by water flow

Through the study of the pressure distribution position, to optimize the design of the structure, make the pressure distribution more uniform. Because it is difficult to study the pressure around the fin when the fin swings in the water, it is necessary to study the pressure on the fin surface generated by the water flow at the normal sailing speed of 2 m/s under static conditions. In order to describe the change of surface pressure during the fin movement, 12 equidistance time points within a cycle were selected for simulation as fig.7.

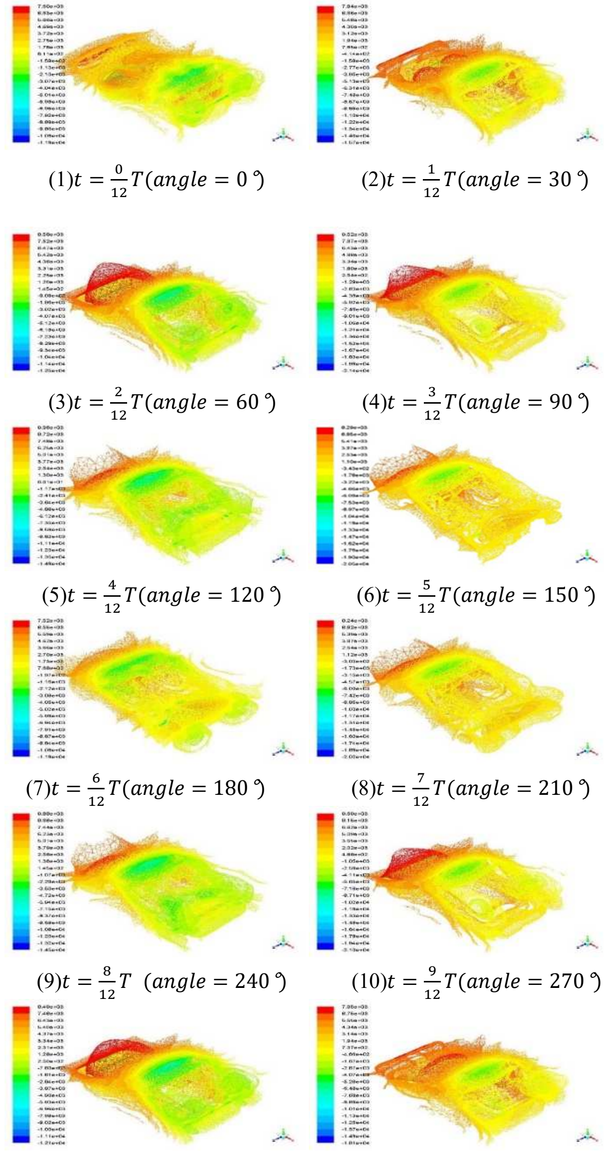

(1)$t = \frac{0}{12}T(angle = 0°)$ (2)$t = \frac{1}{12}T(angle = 30°)$

(3)$t = \frac{2}{12}T(angle = 60°)$ (4)$t = \frac{3}{12}T(angle = 90°)$

(5)$t = \frac{4}{12}T(angle = 120°)$ (6)$t = \frac{5}{12}T(angle = 150°)$

(7)$t = \frac{6}{12}T(angle = 180°)$ (8)$t = \frac{7}{12}T(angle = 210°)$

(9)$t = \frac{8}{12}T\ (angle = 240°)$ (10)$t = \frac{9}{12}T(angle = 270°)$

(11)$t = \frac{10}{12}T(angle = 300°)$ (12)$t = \frac{11}{12}T(angle = 330°)$

Fig. 7 Pressure distribution of 12 fins from different states

As can be seen from the fig.7, the pressure on the surface of the fin is distributed between -20000 and 10000 Pa. It can be seen that the highest positive pressure is generated. By comparing the fish waveforms, it can be seen that when the convex surface area facing the water surface is larger, the positive pressure will be larger, while the negative pressure will be larger at the top of the concave surface facing the water current. According to the pressure distribution, it can be inferred that decreasing the disk diameter and increasing the spacing can effectively reduce the fluctuation on the fin surface and make the pressure distribution more uniform.

B. Flow velocity analysis on the surface of a fish fin

Turbulence has a great influence on the motion and stability of the vehicle, so it is very important to measure the velocity of the current on both sides of the fin. Designing structures where the flow is faster, or changing the material of the fins, can enhance the stability of the whole structure. In order to describe the change of velocity during the fin movement, 12 equidistance time points within a cycle were selected for simulation as fig.8.

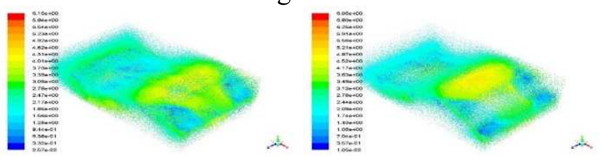

(1)$t = \frac{0}{12}T(angle = 0°)$ (2)$t = \frac{1}{12}T(angle = 30°)$

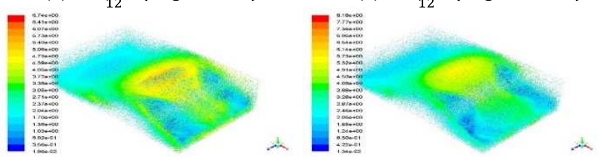

(3)$t = \frac{2}{12}T(angle = 60°)$ (4)$t = \frac{3}{12}T(angle = 90°)$

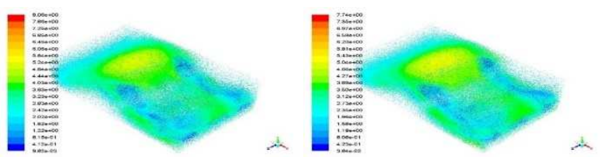

(5)$t = \frac{4}{12}T(angle = 120°)$ (6)$t = \frac{5}{12}T(angle = 150°)$

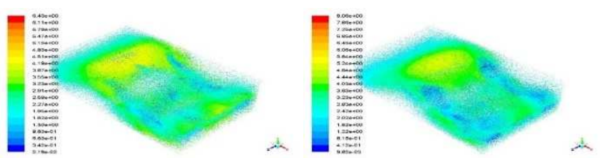

(7)$t = \frac{6}{12}T(angle = 180°)$ (8)$t = \frac{7}{12}T(angle = 210°)$

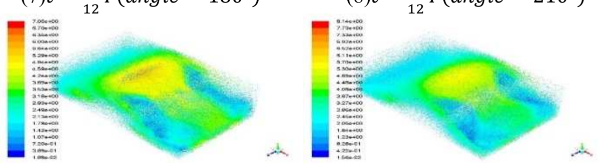

(9)$t = \frac{8}{12}T\ (angle = 240°)$ (10)$t = \frac{9}{12}T\ (angle = 270°)$

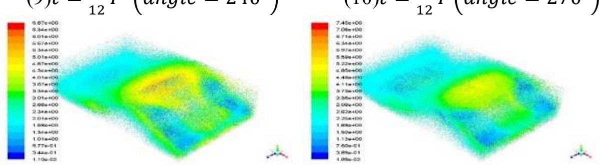

(11)$t = \frac{10}{12}T(angle = 300°)$ (12)$t = \frac{11}{12}T(angle = 330°)$

Fig. 8 Flow velocity distribution of 12 fins from different states

When the included Angle is 90 degrees, the maximum speed is 8.18m/s; when the included Angle is 0 degrees, the maximum speed is 6.15m/s. When the included Angle is 300 degrees, the minimum speed is 0.011m/s, and when the included Angle is 210 degrees, the minimum speed is 0.00982m/s. From these fig.8, it can be seen that the higher velocity is distributed on the top of the convex surface, and the lowest velocity is distributed on the concave surface, even where the water is still. Turbulence has a great influence on the motion and stability of the vehicle, so it is very important to measure the velocity of the current on both sides of the fin. Designing structures where the flow is faster, or changing the material of the fins, can enhance the stability of the whole structure.

C. *Drag analysis of fin surface*

The forces received by all points on the surface of the fin were combined in the X direction to obtain the resistance of the fin in the water flow. The fluid simulation of the fins corresponding to the angles of 0, 30, 60, 90, 120, 150, 180, 210, 240, 270, 300, 330 degrees were carried out to obtain the corresponding 12 groups of resistance. Because the movement of the fin is a cycle, and the Angle change within a cycle is exactly 360 degrees, the pressure and velocity below will also present corresponding periodic changes.

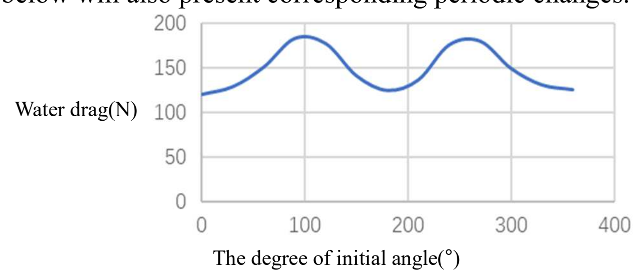

Fig. 9 The relation between water drag and initial angle

It can be seen that the resistance is a sinusoidal function with a period of 180 degrees, with the lowest resistance of 120 N and the highest resistance of 185 N. It can be seen from the image that when the disc crank is parallel to the swing rod, the resistance is the least, and when the crank is perpendicular to the swing rod, the resistance is the largest. By comparing the shape of the fins at different moments, it can be seen that when the fins are symmetrical at the center or on both sides, the resistance is the least and the resistance is about the same at these moments, when the fins are asymmetric, the resistance is greater. This means that we can change the speed of the motor, reduce the speed in the symmetric state, increase the speed in the asymmetric state, and effectively reduce the resistance through the fluctuation of the speed.

D. Analysis of buoyancy on the surface of fish fins

The forces received by all points on the surface of the fin were combined in the Z direction to obtain the resistance of the fin in the water flow.

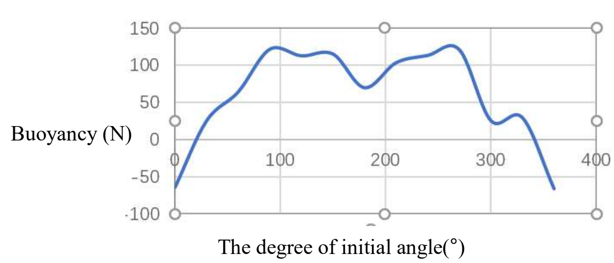

Fig.10 The relation between buoyancy and initial angle

Buoyancy is a cycle of 360 degrees of M shape periodic function, when the Angle of 0 degree, minimum buoyancy, can appear even in the opposite direction downward buoyancy, size of -60 N, when the Angle of 20 degrees and 340 degrees, no buoyancy. We can use different shape of buoyancy to control the size of the vehicle to float up and down.

V. Conclusion

The characteristics of wave-propelled rays were analyzed. An isometric angle multi-linkage skate underwater robot is designed, and the kinematic analysis of the designed mechanism is carried out by using ADAMS simulation software. The kinematic model of the bionic ray was established by observing the movement and mode of the ray's swinging fin in the water.

We can decrease the disk diameter and increase the spacing to reduce the fluctuation on the fin surface and make the pressure distribution more uniform. Designing structures where the flow is faster, or changing the material of the fins, can enhance the stability of the whole structure. we can change the speed of the motor, reduce the speed in the symmetric state, increase the speed in the asymmetric state, and effectively reduce the resistance through the fluctuation of the speed. The new structure can provide a new design idea for the future underwater robot design. In addition, the simulation of pressure and flow velocity can provide us with data reference for the optimization of fins and the improvement of movement mode. In the future, the structure will be slightly adjusted and more external conditions will be added to the simulation.

Acknowledgment

This research was supported by National Natural Science Foundation of China (61773064, 61503028), National Key Research and Development Program of China (2017YFB1304404), and National Hightech Research and Development Program (863 Program) of China (No.2015AA043202).

References

[1] L. Shi and S. Guo, "Development of an Amphibious Turtle-Inspired Spherical Mother Robot," *Journal of Bionic Engineering*, pp. 1702–1707, 2013.

[2] L. Shi, Y. Hu, S. Guo and H. Xing, "A Fuzzy PID Algorithm for a Novel Miniature Spherical Robots with Three-dimensional Underwater Motion Control," *Journal of Bionic Engineering*, vol.17, no.5, pp.959-969,2020.

[3] X. Hou, S. Guo and L. Shi, "Improved Model Predictive-Based Underwater Trajectory Tracking Control for the Biomimetic Spherical Robot under Constraints," *Applied Science*, vol.10, no.22, pp.8106, 2020.

[4] S. Gu, S. Guo and L. Zheng, "A highly stable and efficient spherical underwater robot with hybrid propulsion devices," *Autonomous Robots*, vol.44, no.5, pp.759-771, 2020.

[5] S. Yang, "Design and development of a new kind of pectoral oscillation propulsion robot fish," *Robot*, vol.30, no.6, pp.508-515, 2018.

[6] T. Wang, X. Yang and J. Liang, "A Survey on Bionic Autonomous Underwater Vehicles Propelled by Median and/or Paired Fin Mode," *Robot* , vol.35, no.3, pp.352, 2018.

[7] Y. Wang, J. Tan and D. Zhao, "Design and Experiment on a Biomimetic Robotic Fish Inspired by Freshwater Stingray," *Journal of Bionic Engineering*, vol.12, no.2, pp.204-216, 2019.

[8] Low, "Learning from gymnotiform swimmers—design and implementation of robotic knifefish NKF-II," *International Journal of Information Acquisition*, vol.5, no.2, pp.137-147, 2018.

[9] C. Jing, "Learning Control for Biomimetic Undulating Fins: An Experimental Study," *Journal of Bionic Engineering*, vol.7, no.4, pp. s191-s198, 2020.

[10] J. Chen, "Conception of a Tendon-Sheath and Pneumatic System Driven Soft Rescue Robot," *Advances in Intelligent Systems and Computing*, vol.345, pp. 475-481, 2015.

[11] W. Wu and S. Zhang, "[IEEE 2009 IEEE International Conference on Robotics and Biomimetics (ROBIO) - Guilin, China (2019.12.19-2019.12.23)] 2019 IEEE International Conference on Robotics and Biomimetics (ROBIO) - Design and experimental research on an undulatory robotic fin," *International Conference on Robotics & Biomimetics IEEE*, pp.2440-2444, 2019.

[12] W. Liu, and T. Wang, ""Adaptive refinement scheme for triangular meshes," *Computer Engineering*, vol. 32, pp.14-16, 2006.

[13] M. Theberge and G. Dudek, "Gone swimming seagoing robots," *Spectrum IEEE*, vol.43, no.6, pp.38-43,2015.

[14] T. Toth, and S. Daun, "A three-leg model producing tetrapod and tripod coordination patterns of ipsilateral legs in the stick insect," *Journal of Neurophysiology*, vol.115, no.2, pp.jn.00693.2015.

[15] Nizami, "Proximal Actuation of an Elastically Loaded Scissors Mechanism for the Leg Design of a Quadruped Robot," *IEEE Access*, vol.8, pp.208240-208252, 2020.

[16] S. Zhang, "Initial Development of a Novel Amphibious Robot with Transformable Fin-Leg Composite Propulsion Mechanisms," *Journal of Bionic Engineering*, vol.10, no.4, pp.434-445, 2018.

[17] B. Zhong, "Locomotion Performance of the Amphibious Robot on Various Terrains and Underwater with Flexible Flipper Legs," *Journal of Bionic Engineering*, vol.13, no.4, pp.525-536,2019.

[18] B. Xiao, "Robust Tracking Control of Robot Manipulators with Actuator Faults and Joint Velocity Measurement Uncertainty," *IEEE/ASME Transactions on Mechatronics*, no.99, pp.1-1, 2020.

[19] X. Lin, S. Guo, K. Tanaka and S. Hata, "Development of a spherical underwater robot," *IEEE*, pp.662-655, 2018.

[20] S. Hong, "In-water visual ship hull inspection using a hover-capable underwater vehicle with stereo vision," *Journal of Field Robotics*, vol.36, no.3, 2018.

[21] Z. Zhao, "Computational research on a combined undulating-motion pattern considering undulations of both the ribbon fin and fish body," *Ocean Engineering*, vol.183, no.JUL.1, pp.1-10, 2019.

[22] J. Liang, "2D nonlinear inversion of bedrock motion from the surface motion of a layered half-space," *Engineering Analysis with Boundary Elements*, vol.106, pp.149-159, 2019.